WELDING RESEARCH

SUPPLEMENT TO THE WELDING JOURNAL, JUNE, 1985

Sponsored by the American Welding Society and the Welding Research Council
TECHNICAL PAPERS EDITOR: T.P. SCHOONMAKER

High Temperature Impression Creep Testing of Weldments

The impression creep test technique is capable of monitoring the localized creep resistance of the various microstructural zones in weldments

BY W. S. GIBBS, S. H. WANG, D. K. MATLOCK, AND D. L. OLSON

ABSTRACT. The impression creep test technique, a modified hot hardness test in which the time dependence of the indentor displacement correlates directly to creep properties, has been utilized to measure the localized creep properties across welded joints. High temperature creep data, as a function of position, with respect to the fusion line, were measured on an autogeneous GTA aluminum weld and on an austenitic stainless steel to ferritic steel dissimilar metal weldment.

The creep resistance of the aluminum weld decreased with position on traversing from the solidified weld metal to the base metal, and the variation in creep resistance with position was shown to correlate directly to gradients in microstructure. The creep resistance of the HAZ in the dissimilar metal weldment was shown to decrease with time and correlate to observed cracking in transition joints in fossil fuel power plants. Implications for further application of the impression creep test to weldments are discussed.

Based on a paper presented at the 65th Annual AWS Convention held in Dallas, Texas, during April 8-13, 1984.

W. S. GIBBS is with Allied Bendix Aerospace, Kansas City, Missouri; and S. H. WANG, D. K. MATLOCK, and D. L. OLSON are with the Center for Welding Research, Department of Metallurgical Engineering, Colorado School of Mines, Golden, Colorado.

Introduction

The evaluation of mechanical properties of welded joints has received considerable attention in the past, because weldments are often nucleation sites for catastrophic failures. The process of welding, either during primary fabrication or field repair, results in the development of metallurgical joints with heterogeneous microstructures and properties. The term "heterogeneous" indicates that the microstructures vary with position. This is in direct contrast to wrought base metals, which are assumed to possess essentially homogeneous microstructures and mechanical properties.

Normally, weldment mechanical properties are evaluated with the procedures and sample geometries which were originally designed for metals with homogeneous microstructures. For example, the tensile properties of a weldment can be obtained from standard samples machined either perpendicular or parallel to the centerline of the weld bead. For the transverse sample, the tensile sample gage section contains the complete distribution of weldment microstructures, and the observed deformation behavior is controlled by the weakest zone.

Tensile samples machined parallel to the weld centerline depend on location and may include only weld metal, or may include parallel zones of weld metal, heat affected zone, and base metal. For samples machined parallel to the weld centerline, the observed deformation behavior results from an averaging of the various zones contained in the gage section. These two tensile sample orientations will in general provide different results. Similar difficulties are observed in fracture testing in which the notch and corresponding fracture path, must be specified prior to testing.

Several publications (Refs. 1, 2) have shown that a more complete understanding of the mechanical properties of welded joints can only be achieved if the specific contributions of the zones in the heterogeneous microstructures are considered. As a first approximation, weldments can be viewed as "composite" structures in which the elements of the composite are the different microstructural zones. With an appropriate composite theory and the mechanical properties of the individual zones, it is conceivable that the average mechanical properties of the weldment could be predicted.

The deformation and fracture behavior of individual zones within the heterogeneous weldment are usually evaluated with one of the following two methods: machine sub-sized mechanical test specimens such that the gage length or fracture path includes only material from a specific region within the weldment (Ref. 3); and produce bulk samples with microstructures which simulate those observed at specific locations within the weldment (Ref. 4).

In this paper, a new mechanical test procedure for evaluating the position dependent mechanical properties across a weldment is considered. Specifically, the impression creep test technique developed by Li and his coworkers (Refs. 5-8) is applied to monitor the effects of microstructural gradients on the localized high temperature creep properties in weldments. In the following sections, background information on the impression creep test technique is first presented. Then creep failures, which develop in high temperature dissimilar metal transition joints in power generating systems, are discussed to demonstrate the importance of quantifying the position dependent creep properties across a weldment. Finally, impression creep data on pure aluminum gas tungsten arc (GTA) weldments and austenitic to ferritic dissimilar metal weldments are discussed.

Measurements of Creep and Some Microstructural Effects

Impression Creep Testing

The impression creep test technique (Refs. 5-8) is essentially a modified hot hardness test in which the displacement as a function of time of a cylindrical punch under a constant load (and correspondingly a constant stress) is measured. The punch penetration rate (or impression velocity) is controlled by the time dependence of the movement of mass from under the punch, and thus directly monitors the creep characteristics of a localized zone of material below the punch. Therefore, punch displacement and impression velocities are directly analogous to conventional creep strain and creep rates.

Equivalency between impression creep testing and conventional creep testing is best demonstrated by considering the effects of stress and temperature on the appropriate deformation rates. The stress and temperature dependence of steady state creep has been shown by several investigators (Refs. 9, 10) to follow a unified equation of the following basic form:

$$\dot{\epsilon} = A\sigma^{n_c} \exp(-Q_c/RT) \qquad (1)$$

where $\dot{\epsilon}$ is the steady state creep rate, n_c is the stress exponent for conventional creep, Q_c is the apparent activation energy for conventional creep, A is a structure sensitive constant, and R and T have their usual meaning. In a similar form, Li has shown (Ref. 5) that impression creep velocities, μ, can be described by:

$$\nu = B\left(\frac{\sigma_i}{K}\right)^{n_i} \exp(-Q_1/RT) \qquad (2)$$

where for impression creep, n_i is the stress exponent, Q_i is the apparent activation energy, K is a stress correction factor which accounts for the constraint imposed by the non-deforming material on the deformation zone below the punch, and B is a constant which includes an effective gage length required to correlate punch velocities with creep rates (Ref. 7).

Through an evaluation of the high temperature creep behavior of single crystals and pure polycrystalline materials, Li showed (Refs. 5-7) that $n_i = n_c$ and $Q_i = Q_c$. This comparison indicates that the impression creep test, which monitors the creep behavior of a localized volume of material, can be used to evaluate the creep characteristics of materials.

Microstructural Gradients in Weldments—An Example

An example high temperature application, which illustrates the importance of understanding the local creep properties within a heterogeneous weld zone, is the austenitic to ferritic steel transition joint used in fossil fuel power plant boiler tubes. Dissimilar metal tube joints historically have exhibited poor service life as several service failures have occurred after exposure for times much less than the designed life of 300,000 hours (h) (Ref. 11). In general, failures occur parallel to the fusion line in the 2¼ Cr-1Mo steel at a location one or two grains from the fusion line (Refs. 12, 13). The failures are characteristic creep rupture failures with evidence of grain boundary sliding controlled creep crack growth (Ref. 12). The critical feature of these failures is that the creep crack growth occurs in a specific microstructural band within the microstructural gradient associated with the weld.

Compared to similar metal weldments in which the weld metal composition closely approximates the base metal composition, dissimilar metal weldments more significantly perturb the local microstructures and properties of the welded joint. To illustrate the effects of welding and thermal history on microstructural gradients in dissimilar metal weldments, 2¼ Cr-1Mo steel to Type 316 stainless steel submerged arc welds with Type 310 stainless steel filler metal were prepared as part of this study on impression creep. The resulting microstructural gradients, etched in 2% nital to show the ferritic microstructures, are presented in Fig. 1 for the as-welded condition and in Fig. 2 for a sample aged 120 h at 675°C (1247°F). Based on a Larson-Miller calculation, the 120 h at 675°C (1247°F) simulates approximately one to two years service at a more typical operating temperature of 593°C (1099°F).

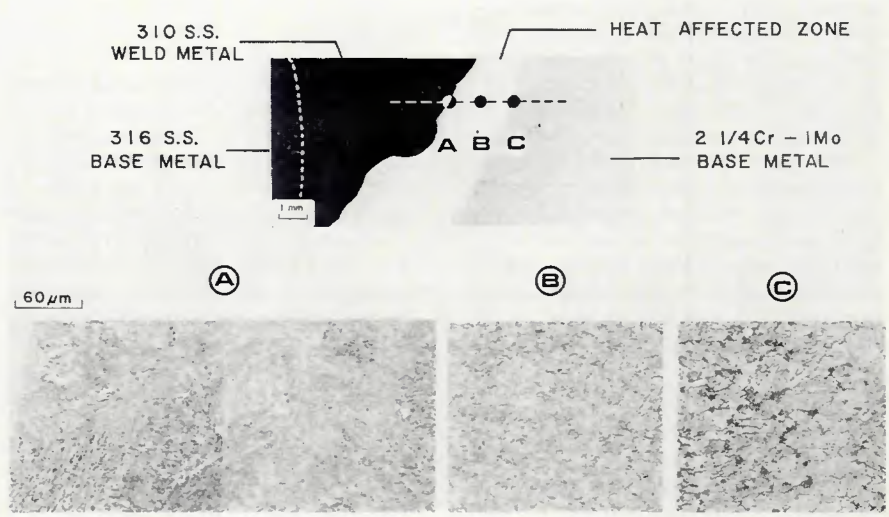

Fig. 1 — As-welded microstructures of a 2¼ Cr-1Mo steel to Type 316 stainless steel dissimilar weldment joined with Type 310 stainless steel filler metal: A — adjacent to the fusion line; B — at approximately 1.1 mm (0.043 in.) from the fusion line; C — at approximately 2.4 mm (0.94 in.) from the fusion line

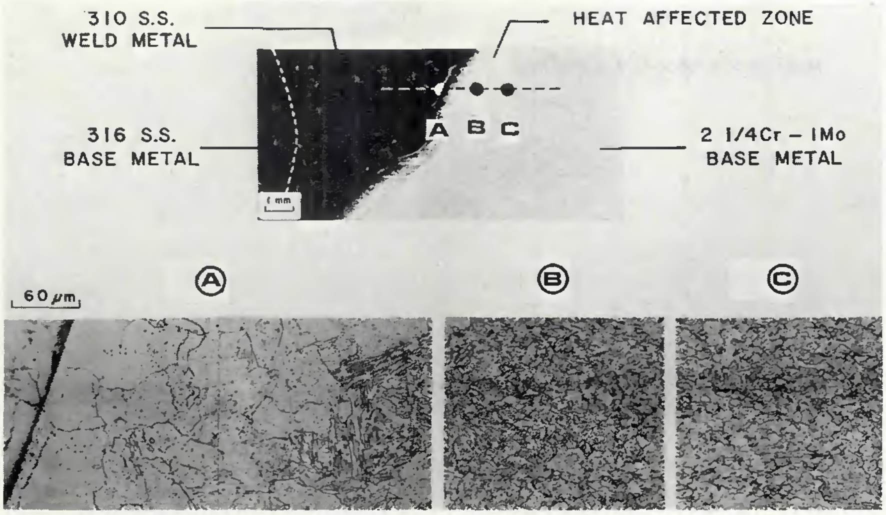

Fig. 2 — Microstructures of a 2¼ Cr-1Mo steel to Type 316 stainless steel dissimilar weldment joint with a Type 310 stainless steel filler metal; weldment was aged 120 h at 675° C (1247°F): A — adjacent to the fusion line; B — at approximately 1.1 mm (0.043 in.) from the fusion line; C — approximately 2.4 mm (0.94 in.) from the fusion line

In the as-welded condition of Fig. 1, the 2¼ Cr-1Mo steel exhibits a microstructural gradient from the weld metal to the base metal. The gradient can be approximated by four sequential regions:

1. Bainite adjacent to the weld pool.
2. Fine-grained proeutectoid ferrite with fine ferrite-carbide aggregates.
3. A partially transformed zone with localized regions of bainite in a matrix which consists of the base plate microstructure in a tempered condition.
4. The tempered base plate microstructure of coarse ferrite with uniformly distributed carbide.

After aging at high temperatures, significant changes to the microstructural gradient develop. First, due to the differences in the chemical potential of carbon in austenite, with respect to carbon in ferrite, carbon diffuses from the 2¼ Cr-1Mo steel to the austenitic weld pool. Adjacent to the fusion line, a carbon depleted zone in the 2¼ Cr-1Mo steel and a carbon-enriched zone at the boundary of the austenitic weld pool develop.

The carbon depleted zone, shown in Fig. 2, consists of large ferrite grains with a low density of uniformly dispersed carbides; while the carbon enriched zone in the austenite exhibits carbides not present in the as-welded condition. Adjacent to the carbon depleted zone in the base metal is a region of large grain ferrite with a higher carbide density. This zone formed from the bainite present on welding and exhibits evidence of the prior bainitic structure. The next zone consists of equiaxed fine grain ferrite with a uniform carbide distribution. The remainder of the plate is tempered base metal with a ferrite grain size intermediate to the coarse and fine grained zones discussed above.

The microstructural gradients which develop due to the combined effects of welding and aging during service correlate directly with observed service failures. Specifically, service failures result from the growth of low ductility grain boundary sliding controlled creep cracks in the carbon depleted, large grain zone (Refs. 11, 13). As an example, Fig. 3 shows a creep crack which developed in service in a dissimilar metal weldment received from the American Electric Power Service Corporation (Ref. 12).

Several studies have shown that the creep cracks in dissimilar metal weldments are a direct result of the high local stresses, which develop in the ferrite due to both the thermal expansion mismatch and the discontinuity in creep resistance between the ferritic base metal and the austenitic weld metal (Refs. 13, 14). In Fig. 3, the loss of creep resistance due to decarburization in the 2¼ Cr-1Mo steel concentrated the creep deformation in a localized zone within the heat-affected zone. Thus, for a proper description of the creep processes associated with the cracking, knowledge of the creep behavior of the zone adjacent to the weld metal is required. In the following sections, results on the application of the impression creep testing technique to the evaluation of localized creep properties in weldments is presented.

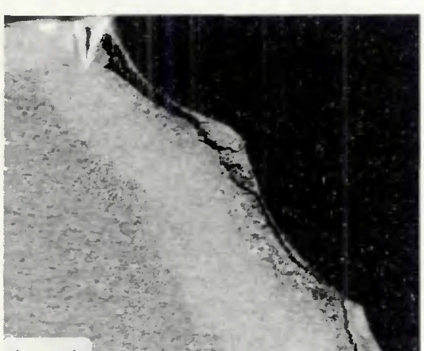

Fig. 3 — An optical micrograph of cracking in the ferritic steel adjacent to the fusion line in a dissimilar metal weldment which experienced 20 years at approximately 500°C (932°F)

Experimental Procedure

An impression creep system (Refs. 5, 6, 7) was constructed within a purified argon-filled glove box. Loads were applied through cylindrical punches of either Al_2O_3 or molybdenum. Al_2O_3 punches were 0.92 mm (0.036 in.) in diameter and were used with the aluminum samples; the molybdenum punches were 1.0 mm (0.04 in.) in diameter and were used with the steel samples. The punches were mounted to a loading rod, guided with linear bearings, and displacements were measured with a linear variable differential transformer (LVDT).

With this system, displacements to $\pm 1 \times 10^{-7}$ m (4×10^{-6} in.) were continuously recorded on a strip chart recorder. The samples with support rod and the punch assembly were contained within a split, resistance wound furnace and temperature was maintained to within ±1°C (1.8°F). Details of the test system are described further by Gibbs (Ref. 15).

Two sets of weldments were used for this study. First, autogeneous gas tungsten arc (GTA) welds on 99.999% aluminum were prepared. These weldments provided samples with a simple microstructural gradient consisting primarily of variations in grain size and grain shape. Prior to welding, the aluminum samples were annealed for 15 minutes (min) at 450°C (842°F). The second set were the 2¼ Cr-1Mo steel to Type 316 stainless steel submerged arc weldments discussed in conjunction with Figs. 1 and 2.

Prior to testing, all impression creep samples were ground flat, to approximately 8 mm (0.31 in.) thick slices, polished with alumina, and lightly etched in 2% nital to reveal the fusion line. Samples were placed into the impression creep system and the temperature was stabilized prior to the application of the creep load.

Results and Discussion

Alumium Weldments

The impression creep properties of the 99.999% aluminum base material were

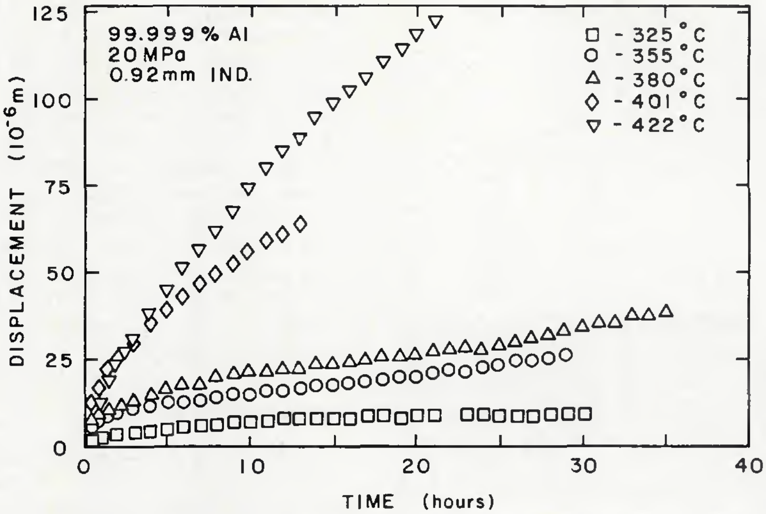

Fig. 4 — Punch displacement vs. time data for 99.999% Al in the temperature range of 325 to 422°C (617 to 792°F) at an impression stress of 20 MPa (2.9 ksi)

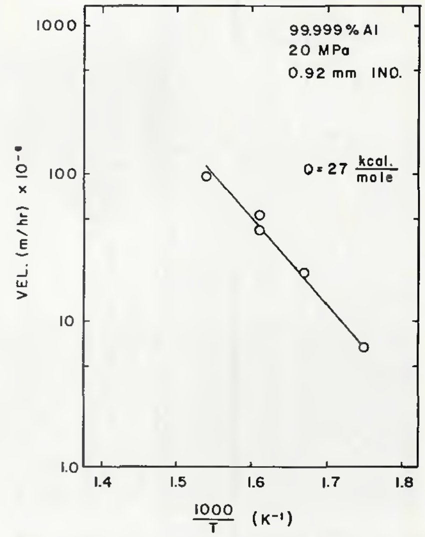

Fig. 5 — Arrhenius analysis of steady state displacement velocities for 99.999% Al samples tested from 325 to 422°C (617 to 792°F)

evaluated as a function of temperature at a constant stress of 20 MPa (2.9 ksi); the resulting displacement-time data are presented in Fig. 4. Similar to normal creep data, the impression creep curves in Fig. 4 suggest a region of primary creep in which the displacement velocity decreases with strain followed by a region of essentially steady-state creep in which the displacement velocity is independent of strain.

The displacement velocities in the steady-state creep regions of Fig. 4 were evaluated according to equation (2) and are shown in Fig. 5, which is a plot of the displacement velocity vs. the inverse of the absolute test temperature. From Fig. 5, an apparent activation energy for impression creep of 27 kcal/mole was determined. This value is in excellent agreement with the values of 28 to 34 kcal/mole of Sherby and Burke (Ref. 9) for normal creep of pure aluminum in the temperature range of 325 to 425°C (617 to 797°F). These data verify the applicability of the impression creep test technique for measuring the creep behavior of polycrystalline material.

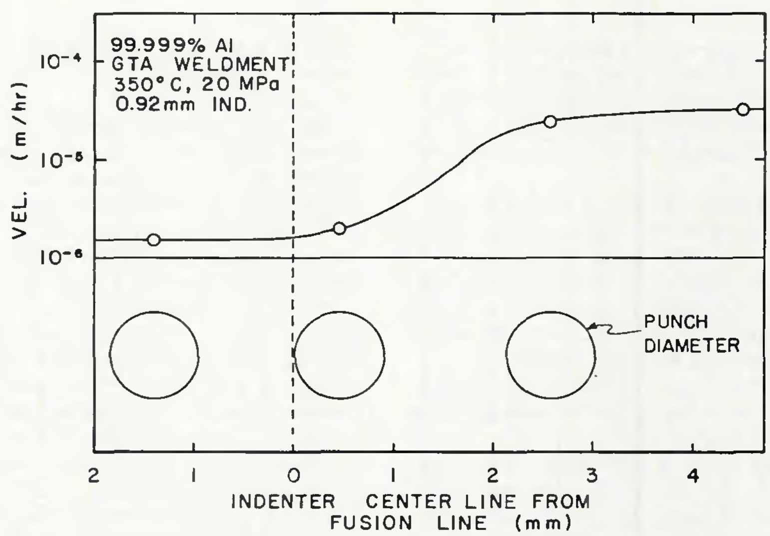

Fig. 6 — Punch velocity vs. distance from the fusion line for 99.999% Al autogeneous GTA weldment; the size of the punch is shown schematically in lower half of the illustration

The impression creep behavior of the 99.999% aluminum GTA weldment was evaluated at 20 MPa (2.9 ksi) and 350°C (662°F). A series of impression creep tests, which represented a traverse from the base metal to the weld metal, were run, and the resulting steady-state impression velocities are plotted in Fig. 6 as a function of position with respect to the fusion line. These results show that the creep resistance of the weld metal, as evidenced by the significantly lower impression creep velocity, is significantly greater than the corresponding base metal. Also there appears to be a gradual transition in creep behavior across the fusion line. For reference, the punch diameter is shown by the large circles on the lower half of Fig. 6.

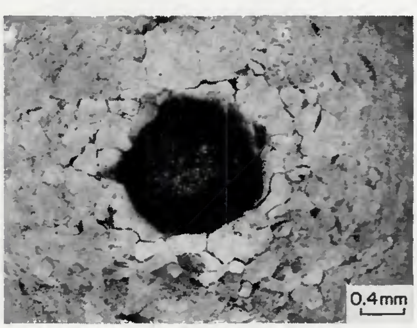

Fig. 7 — Optical photograph of surface deformation for 99.999% Al at 385°C (725°F) for an impression stress of 30 MPa (4.35 ksi); grain boundary sliding can be observed around the punch impression

An understanding of the apparent transition in creep behavior across the fusion line can be obtained from an analysis of the surface deformation morphology around the punch. Optical photographs of the surface deformation are shown in Fig. 7 for the base metal and in Fig. 8 for the punch located adjacent to the fusion line. Due to the constraint of the non-deforming bulk material, plastic flow below the punch is accommodated by surface deformation around the punch.

To illustrate this point, the deformation field around a punch in impression creep is shown in Fig. 9, a schematic drawing of a cross-section through the deformed zone. Figure 9 indicates that the material below the punch must flow radially to accommodate the punch displacement

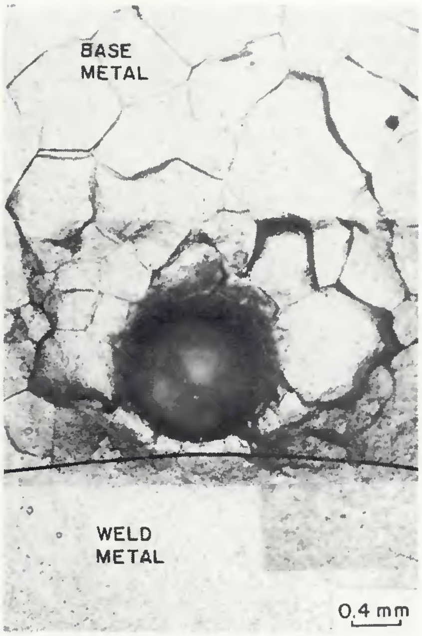

Fig. 8 — Optical photograph of surface deformation in aluminum GTA weldment; the punch is located in the base metal adjacent to the fusion line and deformation is concentrated in the base metal

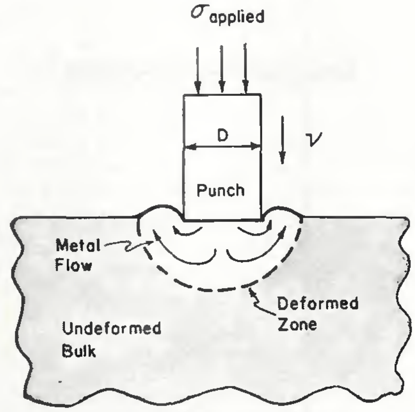

Fig. 9 — A schematic illustration of the deformation field around a punch during impression creep testing

Table 1—Location of Impression Creep Tests in 2¼Cr-1Mo Steel to Type 316 Stainless Steel Weldments

Samples number	Distance from fusion line, (mm)[a]
W1	+3.4
W2	+2.3
W3	+1.7
W4	+0.6
W5	+0.2
W6	−2.4
W7	−5.6

(a) The positive (+) dimensions are measured from the fusion line into the 2¼ Cr-1Mo steel; the negative (−) dimensions are into the weld metals.

and as a result the surface deforms around the punch.

An analysis of Figs. 7 and 8, in conjunction with Fig. 9, indicates that deformation around the punch was uniform in the base metal and nonuniform along the fusion line with deformation concentrated in the base metal. Therefore, the rate of punch penetration is controlled by the distribution of strain in the deformed zone below the punch.

The gradual transition in creep resistance shown in the impression creep traverse of Fig. 6 reflects the composite creep properties of a deformation zone which contains both the creep resistant weld metal and the base metal. The relative volume fractions of the base material and weld metal change with position of the punch, and the observed transition in impression creep properties have been shown (Ref. 15) to follow a simple rule-of-mixtures. The increased creep resistance of the weld metal is attributed to the increased grain size of the columnar grains and the effects of impurity pick-up during the welding operation.

Dissimilar Metal Weldments

Impression creep tests of the 2¼Cr-1Mo steel to Type 316 stainless steel weldments shown in Fig. 1 were measured as a function of position at 675°C (1247°F) with an applied stress of 172 MPa (24.9 ksi). Data were obtained at the positions indicated in Table 1 and a new as-welded sample was used for each test. The resulting punch displacement vs. time data are presented in Fig. 10. These data appear similar to normal creep curves and clearly vary with position.

From the displacement-time data, average impression velocities were obtained, both at the beginning of the test (one hour) and during the apparent steady state region between 50 to 100 h. The initial velocities reflect the as-welded starting microstructure, *i.e.*, Fig. 1, while the average velocities between 50 to 100 h directly measure the effects of the aged microstructures in Fig. 2.

These velocities are plotted in Fig. 11 for data obtained with a 1 mm (0.04 in.) diameter punch and show a significant decrease in creep resistance from the austenitic weld metal to the ferritic base metal. In addition, the minimum creep resistance, *i.e.*, the maximum impression velocity for both the as-welded and aged condition occurs within the microstructural gradient of the heat-affected zone. Furthermore, these data clearly show that the creep properties of the heat affected zone are significantly degraded with aging at high temperatures. This observa-

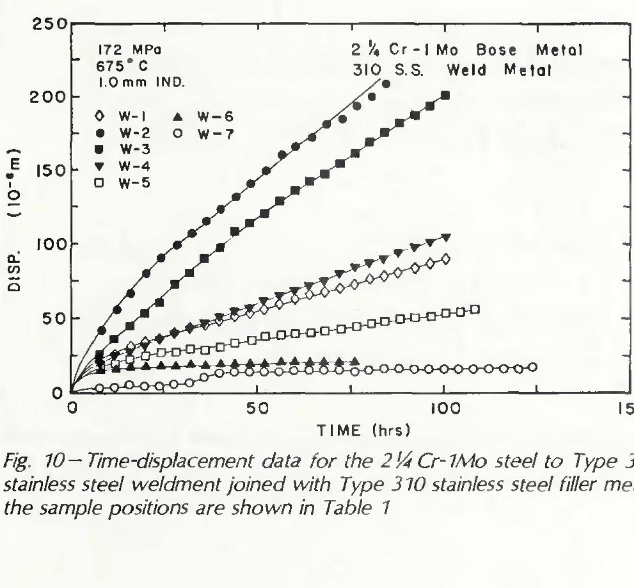

Fig. 10 — Time-displacement data for the 2¼Cr-1Mo steel to Type 316 stainless steel weldment joined with Type 310 stainless steel filler metal; the sample positions are shown in Table 1

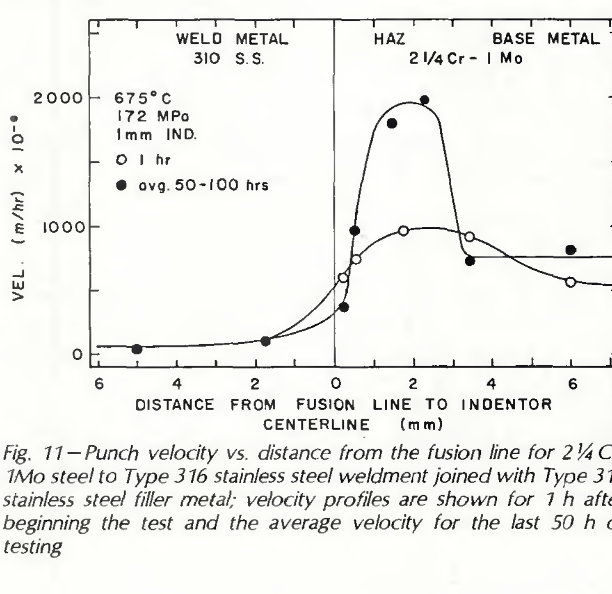

Fig. 11 — Punch velocity vs. distance from the fusion line for 2¼Cr-1Mo steel to Type 316 stainless steel weldment joined with Type 310 stainless steel filler metal; velocity profiles are shown for 1 h after beginning the test and the average velocity for the last 50 h of testing

tion is consistent with the development of the decarburized zone adjacent to the fusion line and the corresponding microstructural gradient shown in Fig. 2 and with the development of the heat affected zone cracking shown in Fig. 3.

As shown in the previous analysis of creep in GTA aluminum weldments, the individual impression velocities within the heat-affected zone represent an average creep resistance of the microstructural gradient below the punch. Thus, adjacent to the fusion line in aged material, the apparent increase in creep resistance (*i.e.,* decrease in impression velocity), when the fusion line is approached from the base metal, reflects the combined effects of increased contributions of the creep resistant austenitic weld metal and the gradients in creep resistance of the decarburized base metal. Adjacent to the fusion line the creep resistance of the ferritic base metal should be lowest (Ref. 16); however, due to the constraint effects imposed by the weld metal, the apparent creep resistance is high.

Conclusions

This study has demonstrated the applicability of the impression creep test technique to evaluating the position dependent creep properties associated with microstructural gradients developed in welding. Transition in creep properties were observed in an autogeneous GTA aluminum weld and in an austenitic stainless steel to ferritic steel dissimilar metal weldment. Furthermore, in the dissimilar metal weldment, the minimum in creep resistance was shown to occur in a zone adjacent to the fusion line where creep cracking has been observed to develop in service.

Further studies on impression creep testing are required in order to refine the test procedures for weldments and data analysis. Improved data on localized microstructures could be obtained with smaller diameter punches. In addition, it is conceivable that portable impression creep systems could be developed to evaluate in-situ creep properties of high temperature system components.

Acknowledgments

This work was supported by the DMS-BES office of the United States Department of Energy.

References

1. Tanaka, K., Sato, M., and Ishikawa, T. 1982. Fatigue COD and short crack arrest tests. International Conference on Fracture Toughness Testing Methods, Interpretation and Analysis. The Welding Institute, London, June, 1982.

2. Zemzin, V. N., and Boikova, K. I. 1982. Cracking resistance of welded joints in dissimilar steels, part I: effect of mechanical heterogeneity of the welded joint. *Svar. Proiz.* 5:4-7.

3. Cavdenas, C., Pense, A. W., and Stout, R. D. 1979. The fracture toughness of a high strength Ni-Cr-Mo alloy steel weldment. *Applications of materials for pressure vessels and piping,* ed. George V. Smith, pp. 137-151. New York: ASME.

4. Alberry, P. J., and Jones, W. K. C. 1977 (January). Comparison of mechanical properties of 2Cr-Mo and 0.5Cr-Mo-V simulated heat-affected zones. *Metals Technology:* 45-51.

5. Chu, S. N. G., and Li, J. C. M. 1977. Impression creep; a new creep test. *J. of Materials Science* 12:2200-2208.

6. Chu, S. N. G., and Li, J. C. M. 1979. Impression creep of β-tin single crystals. *Materials Science and Engineering* 39:1-10.

7. Yu, E. C., and Li, J. C. M. 1977. Impression creep of LiF single crystals. *Phil. Mag.* 36(4):811-825.

8. Yu, H. Y., and Li, J. C. M. 1977. Computer simulation of impression creep by the finite element method. *J. of Materials Science* 12:2214-2222.

9. Sherby, O. D., and Burke, P. M. 1967. Mechanical behavior of crystalline solid at elevated temperature. *Progress in Materials Science* 13(7):325-390.

10. Garafalo, F. 1965. *Fundamentals of creep and creep-rupture in metals,* p. 67. New York: The MacMillan Company.

11. Klueh, R. L., and King, J. F. 1980. *Ferritic-austenitic transition joint failures.* Oak Ridge National Laboratory, ORNL-5637, April, 1980.

12. Campbell, G. M., Elmer, J. W., Gibbs, W. S., Matlock, D. K., and Olson, D. L. 1982. Evaluation of factors controlling high temperature service life of 2¼ Cr-1Mo steel to austenitic stainless steel weldments. *Trends in welding research in the United States,* ed. S.A. David, pp. 443-470. Metals Park, Ohio: American Society for Metals.

13. King, J. F. 1979. *Behavior and properties of welded transition joints between austenitic stainless steels and ferritic steels—a literature review.* Oak Ridge National Laboratory, ORNL-TM-5163.

14. Tucker, Jr., J. T., and Eberle, F. 1956. "Development of a ferritic-austenitic weld joint for steam plant applications. *Welding Journal* 35(11):529-s to 540-s.

15. Gibbs, W. S. 1983. *High temperature impression creep of weldments.* M.S. Thesis, Colorado School of Mines, T-2723.

16. Nath, B. 1982. Creep rupture and creep crack growth behavior of transition joints. *Welding technology for energy applications,* eds. S. A. David and G. M. Slaughter, p. 597. Oak Ridge National Laboratory.

—A Reminder to Authors—

Application forms for presentation of technical papers in the 1986 AWS Convention Professional Program must be postmarked no later than **August 1, 1985.** Be sure to send your application forms and 500–1000 word summaries in on time to ensure consideration for the 67th Annual AWS Convention, to be held April 13–18, 1986, in Atlanta, Ga.

A tear-out Author Application Form can be found in the May, 1985, issue of the *Welding Journal.* For additional applications, contact: Mr. T. P. Schoonmaker, Technical Papers Editor, American Welding Society, P. O. Box 351040, Miami, FL 33135; telephone (305) 443-9353.